ARTICLES

SAP-controlled T–B cell interactions underlie germinal centre formation

Hai Qi[1]*, Jennifer L. Cannons[2]*, Frederick Klauschen[1], Pamela L. Schwartzberg[2] & Ronald N. Germain[1]

Generation of long-term antibody-mediated immunity depends on the germinal centre reaction, which requires cooperation between antigen-specific T and B lymphocytes. In human X-linked lymphoproliferative disease and its gene-targeted mouse model, loss-of-function mutations in signalling lymphocyte activation molecule-associated protein (SAP, encoded by *SH2D1a*) cause a profound defect in germinal centre formation by an as yet unknown mechanism. Here, using two-photon intravital imaging, we show that SAP deficiency selectively impairs the ability of $CD4^+$ T cells to stably interact with cognate B cells but not antigen-presenting dendritic cells. This selective defect results in a failure of antigen-specific B cells to receive adequate levels of contact-dependent T-cell help to expand normally, despite $Sap^{-/-}$ T cells exhibiting the known characteristics of otherwise competent helper T cells. Furthermore, the lack of stable interactions with B cells renders $Sap^{-/-}$ T cells unable to be efficiently recruited to and retained in a nascent germinal centre to sustain the germinal centre reaction. These results offer an explanation for the germinal centre defect due to SAP deficiency and provide new insights into the bi-directional communication between cognate T and B cells *in vivo*.

The germinal centre (GC) reaction, which supports antibody affinity maturation and the generation of B-cell memory[1–3], requires activation of $CD4^+$ T cells by antigen-bearing dendritic cells (DCs), followed by differentiation of these T cells and their physical interactions with antigen-activated B cells[4]. The activated T cells promote the survival, proliferation and differentiation of the B cells by delivering contact-dependent helper signals in an antigen-specific fashion[5–8]. Follicular helper T (T_{FH}) cells, a subset of activated $CD4^+$ T cells that highly express the chemokine receptor CXCR5, the costimulatory molecules CD40L and ICOS, and SAP, are particularly important for a sustained GC response[9].

In human X-linked lymphoproliferative disease and its gene-targeted mouse model, lack of functional SAP protein in T cells causes a profound defect in GC formation and humoral immunity[10–17], but how SAP regulates the GC-promoting T-helper cell response is unknown. An intracellular adaptor protein, SAP binds to signalling lymphocyte activation molecule (SLAM) and other transmembrane molecules of the SLAM family[18,19]. It modulates T-cell antigen receptor signalling and promotes type 2 T helper (T_H2) cell differentiation[13,14,20]. However, impaired T_H2 differentiation alone is not an adequate explanation for the profound GC defect seen in SAP-deficient animals[17,21,22]. To better understand how SAP deficiency results in impaired GC formation, we took a combined approach of classical cellular immunology and intravital two-photon imaging, which allowed us to examine not only the activation phenotype of T cells but also the dynamics of their critical interactions with DCs and B cells *in vivo*[23].

Normal activation of $Sap^{-/-}$ T cells by DCs

Because optimal T-cell activation and differentiation *in vivo* require long-lasting T–DC conjugation[24–27], we first examined the impact of SAP deficiency on T–DC interactions using OT-2 TCR transgenic T cells specific to $I\text{–}A^b$ complexed with an ovalbumin-derived peptide (OVA_{323}). Behaviour of $Sap^{-/-}$ and $Sap^{+/+}$ T cells in the same draining lymph node were compared after co-transfer into mice previously injected subcutaneously with OVA_{323}-pulsed DCs. $Sap^{-/-}$ and $Sap^{+/+}$ OT-2 T cells showed equivalent contact times with DCs presenting OVA_{323} (Fig. 1a, b and Supplementary Movie 1). Consistent with this result, $Sap^{-/-}$ and $Sap^{+/+}$ OT-2 T cells proliferated and accumulated to a similar extent (Fig. 1c). Within the expanded pool of activated T cells of either genotype, similar frequencies of $CXCR5^+ICOS^+$ T_{FH} precursors were observed and both groups of T cells migrated into the B-cell follicular areas of the lymph node (Fig. 1d, e). These data indicate SAP deficiency does not grossly alter initial T-cell interaction with or activation by antigen-presenting DCs *in vivo*.

Selective defect in T–B cell interactions

During a T-dependent B-cell response, helper T cells activated by DCs must subsequently engage antigen-triggered B cells based on class II major histocompatibility complex (MHC class II)-restricted antigen recognition[7,28]. This process is characterized by long-lasting, mobile conjugate pairs formed between cognate T cells and B cells[29]. On the basis of these previous observations, we used intravital imaging to assess whether SAP deficiency affects antigen-dependent T–B cell interactions *in vivo*. $Sap^{-/-}$ and $Sap^{+/+}$ OT-2 T cells were co-transferred into mice together with wild-type B cells expressing the MD4 transgenic B-cell receptor, which recognizes hen egg lysozyme (HEL). As antigen, cross-linked conjugates of HEL and OVA (HEL–OVA) were used to allow activation of both T and B transgenic cells and to permit MHC-class-II-dependent antigen presentation to the OT-2 T cells by the MD4 B cells. After immunization, $Sap^{+/+}$ OT-2 T cells engaged migrating MD4 B cells and formed long-lasting mobile conjugate pairs, whereas $Sap^{-/-}$ OT-2 T cells showed predominantly brief contacts with the same cohort of MD4 B cells (Fig. 2a, b and Supplementary Movies 2 and 3; mean ± s.e.m. of the median T–B cell contact time by $Sap^{+/+}$ versus $Sap^{-/-}$ T cells: 19.2 ± 2.6 versus 8.2 ± 1.9 min, 5 experiments). Thus in notable contrast to the lack of significant effects on the duration of T–DC interactions (Fig. 1a, b),

[1]Lymphocyte Biology Section, Laboratory of Immunology, National Institute of Allergy and Infectious Diseases, National Institutes of Health, Bethesda, Maryland 20892, USA.
[2]Genetic Disease Research Branch, National Human Genome Research Institute, National Institutes of Health, Bethesda, Maryland 20892, USA.
*These authors contributed equally to this work.

the absence of SAP expression in T cells severely reduces the longevity of T–B cell interactions *in vivo*.

To examine more quantitatively the differential effect of SAP deficiency on T–antigen-presenting cell (APC) interactions, a flow-cytometry-based *in vitro* assay was used in which shear stress was imposed on unfixed conjugates between activated OT-2 T-cell blasts and OVA_{323}-pulsed DCs or activated B cells. Whereas a dose-dependent increase in T–B cell conjugate efficiency was observed with $Sap^{+/+}$ OT-2 T cells, such conjugate formation by $Sap^{-/-}$ T cells was low at all peptide concentrations tested (Fig. 2c, left panel). In contrast, within the same non-saturating peptide dose range, $Sap^{-/-}$ T cells were as efficient as wild-type T cells in forming conjugates with DCs (Fig. 2c, right panel). To determine whether the defective adhesion to B cells by activated $Sap^{-/-}$ T cells might have been programmed during their priming interactions with DCs and whether SAP expression is specifically required during T–B cell interactions, DNA constructs encoding either green fluorescent protein (GFP) or a GFP–SAP fusion protein were independently transfected into $Sap^{-/-}$ T-cell blasts. Complementation with GFP–SAP but not GFP alone fully rescued T–B cell conjugate formation by transfected $Sap^{-/-}$ T-cell blasts (Fig. 2d; also see Supplementary Fig. 1). Thus, the requirement for SAP expression in T cells for optimal adhesion to B cells is contemporaneous with T–B cell interaction. SAP facilitates the recruitment of FYN kinase to cytoplasmic tails of SLAM-related proteins, which is important for SAP regulation of T_H2 cytokine production[20,30] but less so for SAP-controlled GC development[17,31].

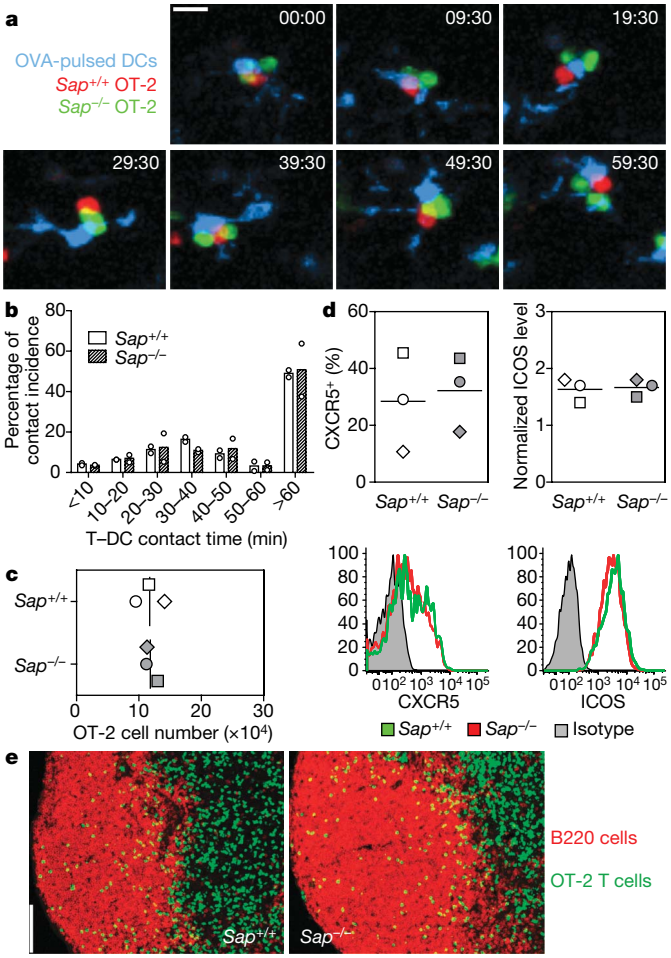

Figure 1 | $Sap^{-/-}$ T cells normally interact with and are activated by DCs *in vivo*. **a**, Time-lapse images of $Sap^{+/+}$ and $Sap^{-/-}$ OT-2 T cells interacting with OVA_{323}-pulsed DCs *in vivo* (see also Supplementary Movie 1). Scale bar, 10 μm. Time is shown in min:s. **b**, Distribution of T–DC contact durations (circles, individual experiments; bars, means). A total of 232 and 224 contacts were scored for $Sap^{+/+}$ and $Sap^{-/-}$ T cells, respectively. **c–e**, T-cell activation phenotypes 96 h after transfer into recipients of OVA_{323}-pulsed DCs. Absolute numbers of OT-2 cells (**c**) and typical patterns of CXCR5 and ICOS expression (**d**). Individual symbols, mean of 3–4 mice per group per experiment; lines, mean of the 3 experiments. **e**, The distribution of activated T cells in B-cell follicles, representative of three experiments. Scale bar, 100 μm.

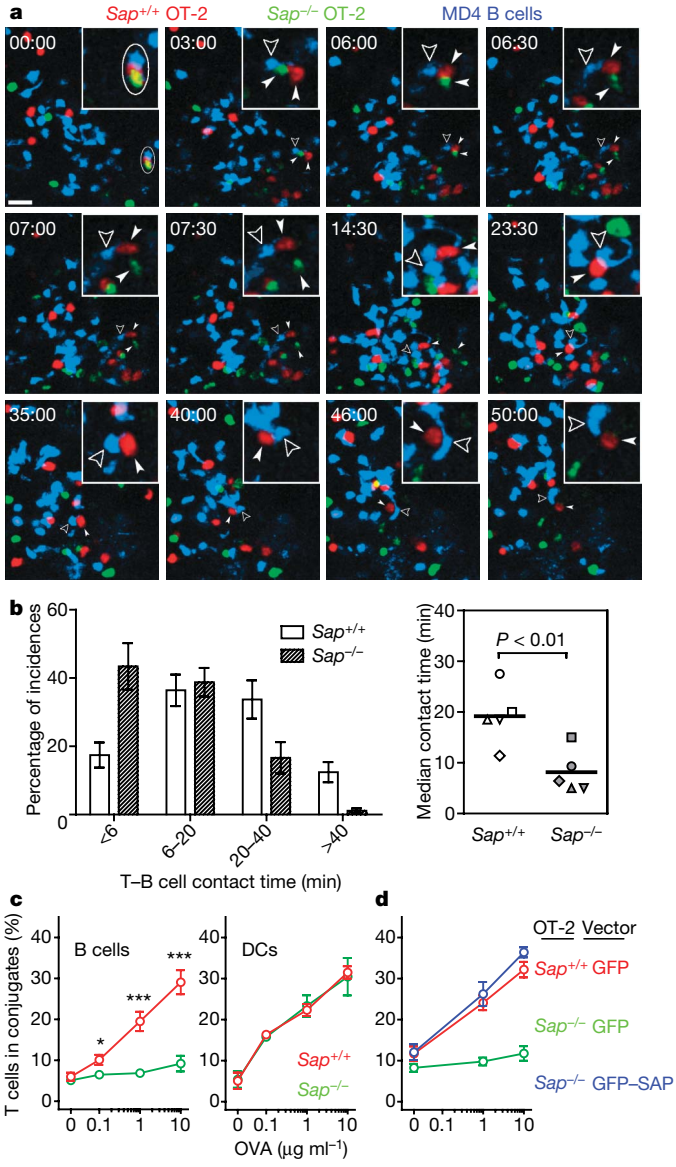

Figure 2 | $Sap^{-/-}$ T cells are defective in adhesion to cognate B cells. **a**, Time-lapse images of $Sap^{+/+}$ and $Sap^{-/-}$ T cells interacting with MD4 B cells 24–36 h after HEL–OVA immunization. Circle, a cell cluster omposed of one $Sap^{+/+}$ and one $Sap^{-/-}$ T cell in contact with the same MD4 B cell at time zero. Solid arrowheads follow the two T cells, and open arrowheads highlight the B cell. Insets show the MD4 cell and its immediate surrounding (see also Supplementary Movie 2). Scale bar, 20 μm. **b**, Left, distribution of contact durations between T cells and MD4 B cells (mean ± s.e.m. of 5 experiments; 190 and 173 contacts scored for $Sap^{+/+}$ and $Sap^{-/-}$ T cells, respectively). Right, the median durations of T–B cell contacts measured in individual experiments. Line, mean of the 5 medians. **c**, Conjugation efficiency of $Sap^{+/+}$ or $Sap^{-/-}$ OT-2 T cells with OVA_{323}-pulsed B cells (left) or DCs (right), expressed as mean ± s.e.m. frequencies of $CD4^+CD19^+$ or $CD4^+CD11c^+$ conjugates in total $CD4^+$ events (5 experiments; asterisk, $P < 0.05$; triple asterisk, $P < 0.001$; see representative cytometry plots in Supplementary Fig. 1). **d**, T–B conjugation assays were conducted using OT-2 cells transiently transfected with DNA constructs expressing either GFP or GFP-tagged SAP as indicated. Frequencies measured in 6 independent experiments are presented as mean ± s.e.m. (also see Supplementary Fig. 1).

Consistent with these latter results, we found that SAP(R78A), a mutant SAP capable of binding SLAM-related molecules but severely impaired in binding FYN kinase[12], rescued T–B cell conjugate formation *in vitro* (Supplementary Fig. 2). Taken together, our analyses of T–APC conjugation establish that SAP critically regulates the contact duration and the adhesive strength of cognate T–B cell but not antigen-driven T–DC interactions.

B cells do not acquire sufficient help

The cell numbers used in the preceding experiments can result in competition among T cells for antigen on presenting cells *in vivo*[32], raising the question of whether $Sap^{-/-}$ T cells would, if present alone, form more stable contacts with antigen-specific B cells or provide B cells with a summed contact time from sequential brief interactions comparable to the total interaction time with wild-type T cells. To examine these issues, small numbers (6×10^4) of $Sap^{+/+}$ or $Sap^{-/-}$ OT-2 T cells were separately transferred into recipient B6 mice that concomitantly received 3×10^5 MD4 B cells. Cumulative interactions between B and T cells were assessed by continuous intravital imaging over a 3-h period of time between 60 h and 72 h post-immunization, when substantial clonal expansion has begun and physical co-localization of activated T and B cells can be observed[8,29,33,34]. Under these modified conditions, $Sap^{-/-}$ OT-2 cells still demonstrated abbreviated contacts with activated MD4 B cells after immunization with HEL–OVA (2.1 ± 0.2 min (mean ± s.e.m.) versus 8.9 ± 0.8 min for $Sap^{+/+}$ T cells, $P < 0.0001$; Fig. 3a and Supplementary Movie 4). Whereas many contacts involving $Sap^{-/-}$ T cells were brief and similar to non-cognate T–B cell contacts in duration, on the population level they lasted for a statistically longer period of time (2.1 ± 0.2 versus 1.3 ± 0.1 min for non-cognate interactions, $P = 0.0014$), indicating that antigen-specific interactions occurred between $Sap^{-/-}$ OT-2 cells and MD4 B cells but were not sustained. Individual B cells were also tracked for their interactions with different T cells. MD4 cells often accumulated >1 h of interactions with $Sap^{+/+}$ OT-2 T cells, whereas they were rarely able to accumulate more than 20 min of contact with $Sap^{-/-}$ OT-2 T cells over the same period (Fig. 3b–d and Supplementary Movies 4 and 5). B cells remained equally trackable under the two conditions and interacted with similar numbers of $Sap^{-/-}$ or $Sap^{+/+}$ T cells (Supplementary Fig. 3). The marked reduction in cumulative time

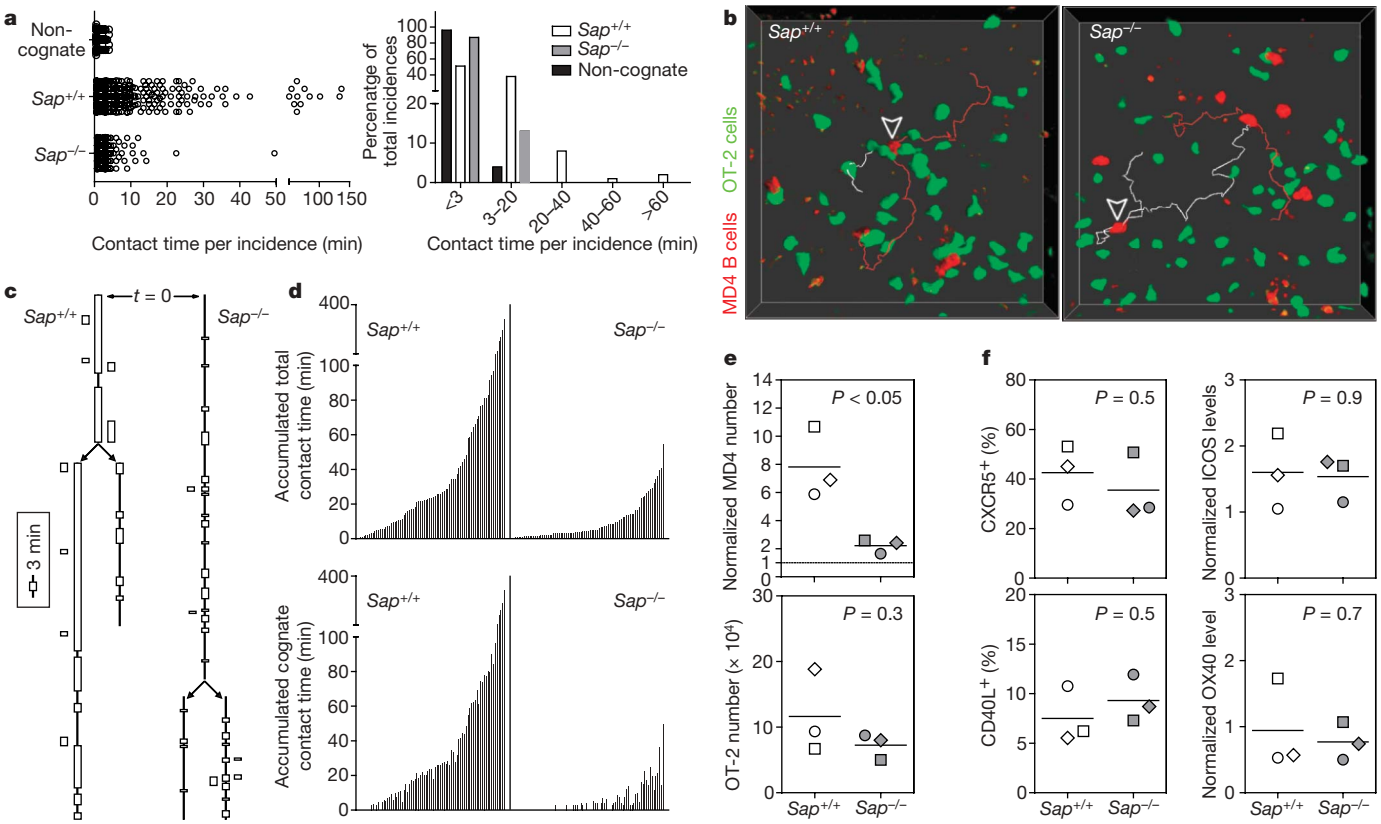

Figure 3 | B cells fail to receive contact-dependent help from SAP-deficient T cells. **a**, Individual T–B contact durations (left) and their distribution (right). Non-cognate conditions involve $Sap^{+/+}$ OT-2 cells non-specifically interacting with MD4 B cells after immunization with HEL–BSA mixed with OVA protein (137 measurements from 2 experiments). Cognate conditions involve specific interactions between $Sap^{+/+}$ or $Sap^{-/-}$ OT-2 T cells and MD4 B cells after immunization with HEL–OVA (380 and 390 measurements from 3 experiments, respectively). **b–d**, Individual MD4 B cells tracked for cumulative interactions with OT-2 T cells over 3 h. **b**, Examples of tracked MD4 cells (arrowheads). MD4 cells represented by white tracks divided during the imaging period; daughter cells are represented by red tracks. **c**, Interaction histories of the MD4 cells in **b**. Vertical lines indicate the periods during which the B cells were present in the imaged volume. Arrows indicate cell divisions giving rise to daughter cells. Boxes represent one contact with a T cell; height indicates the contact duration (see also Supplementary Movie 5). Adjacent boxes indicate simultaneous interactions with more than one T cell. **d**, MD4 cells in each condition tracked in 3 experiments (82 total). Each bar represents one MD4 cell. Bar heights are the sum of all T-cell contacts (top) or only those contacts longer than 3 min (bottom), a cut-off differentiating cognate from non-cognate T–B interactions with a 95% confidence as determined in **a**. **e**, **f**, MD4 B cells (7-amino-actinomycin D (7-AAD)$^-$CD19$^+$IgM^{a+}CD4$^-$GFP$^-$ singlet events) and OT-2 T cells (7-AAD$^-$CD19$^-$CD4$^+$GFP$^+$ singlet events) analysed by FACS in 3 experiments at 96 h post HEL–OVA immunization. Individual symbols (open, $Sap^{+/+}$; filled, $Sap^{-/-}$), mean of 3–4 mice per group per experiment; lines, mean of the 3 experiments. **e**, Cell expansion. Top, numbers of MD4 cells recovered after co-transfer of $Sap^{+/+}$ or $Sap^{-/-}$ OT-2 T cells were normalized against the number obtained when no exogenous OT-2 cells were co-transferred (line at unit 1). Bottom, absolute numbers of recovered OT-2 cells after co-transfer with B cells. **f**, Surface expression of CXCR5, CD40L, ICOS and OX40 by the two types of OT-2 T cells. See Methods for details of quantitative analysis and Supplementary Fig. 4 for representative cytometry plots.

of contact with *Sap*$^{-/-}$ OT-2 T cells correlated with a pronounced impairment of MD4 B cell clonal expansion (Fig. 3e). Nonetheless, *Sap*$^{-/-}$ OT-2 T cells expanded comparably to their *Sap*$^{+/+}$ counterparts and expressed similar levels of CD40L, ICOS, OX40 and CXCR5 (Fig. 3e, f and Supplementary Fig. 4) at this time. The latter is a phenotype considered characteristic of activated T cells capable of effectively promoting humoral responses and with features of T_{FH} precursor cells as commonly defined[9,35]. In combination with the previous data, these findings suggest that it is not an intrinsic inability of SAP-deficient T cells to express key molecular signals, but rather a failure to exchange these signals during sufficiently long periods of contact with B cells, that accounts for their markedly reduced capacity to promote B-cell expansion and subsequent GC development.

Limited recruitment to and retention in GCs

Recruitment of helper T cells to a forming GC is necessary for maintaining the GC reaction[36], and GC-localized T_{FH} cells are required for effective immunoglobulin class switching and antibody affinity maturation[9]. To explore whether SAP deficiency also impairs T-cell recruitment to and retention within nascent GCs, we transferred equal numbers (3×10^4) of cyan fluorescent protein (CFP)-expressing *Sap*$^{+/+}$ OT-2 cells and GFP-expressing *Sap*$^{-/-}$ OT-2 cells into B6 mice together with 3×10^5 non-fluorescent MD4 cells. Six to eight days after HEL–OVA immunization, GCs developed within the draining lymph node, seen as GL7$^+$ (LY77$^+$) areas that largely excluded immunoglobulin D$^+$ (IgD$^+$) naive B cells (Supplementary Fig. 5). Whereas the IgD$^+$ follicular mantle zone was populated by both *Sap*$^{+/+}$ and *Sap*$^{-/-}$ OT-2 cells, the GC area predominantly contained *Sap*$^{+/+}$ OT-2 cells, consistent with a failure of GC recruitment and/or retention of *Sap*$^{-/-}$ T cells.

To examine this issue dynamically, recipient mice were also given dye-labelled naive B cells 24 to 48 h before intravital imaging to differentiate follicular mantle and GC areas. Although individual naive B cells migrate in and out of GCs[37], as a population they remain substantially excluded from GCs (Supplementary Fig. 5), allowing simultaneous identification of the follicular area and approximation of the GC–mantle border using time-averaged images (see Supplementary Fig. 6 for details). *Sap*$^{+/+}$ and *Sap*$^{-/-}$ OT-2 T cells exhibited markedly different dynamic patterns within the follicle (Fig. 4a and Supplementary Movie 6). Whereas *Sap*$^{+/+}$ OT-2 T cells migrated freely into and accumulated within the GCs, *Sap*$^{-/-}$ OT-2 T cells mainly swarmed in the follicular mantle. To quantify migratory behaviours of the two types of T cells around GCs, a tessellation algorithm was used to reconstruct the GC surface (Supplementary

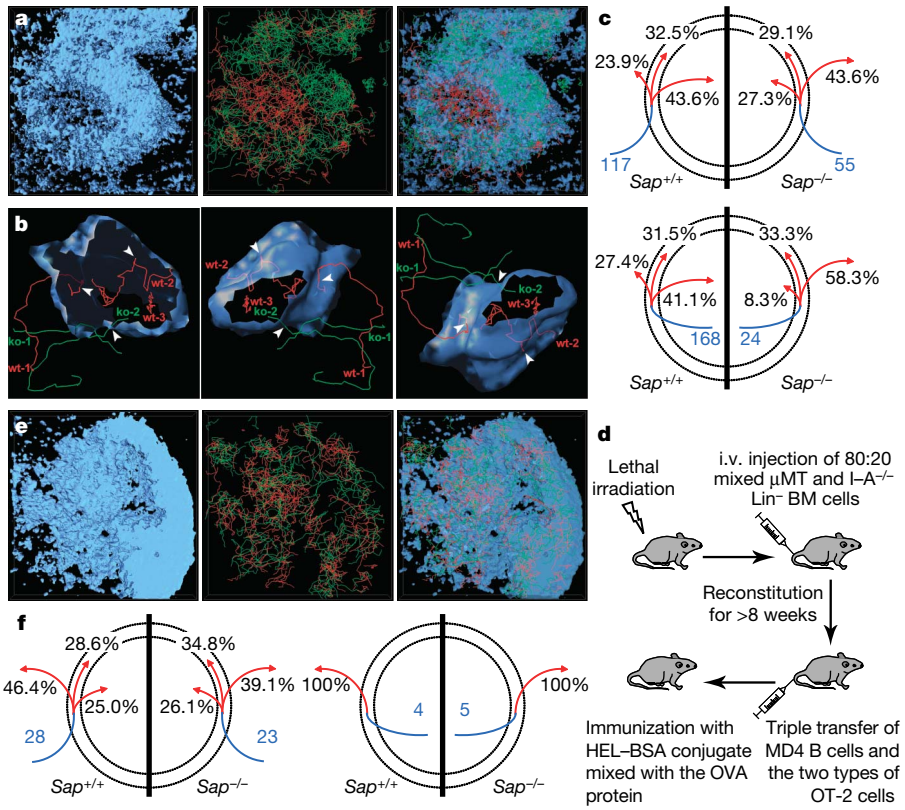

Figure 4 | Defective GC recruitment and retention of *Sap*$^{-/-}$ T cells due to lack of efficient cognate interactions with B cells. **a**, Typical migration patterns of *Sap*$^{+/+}$ (red) and *Sap*$^{-/-}$ (green) OT-2 T cells in follicles containing cognate GCs. Left, the naive B-cell-dominated follicular mantle zone encasing GC area (see Supplementary Fig. 6 for details of three-dimensional rendering); middle, distribution of migration tracks of OT-2 T cells; right, overlay with the mantle zone rendered as semi-transparent (see also Supplementary Movie 6). **b**, GC surface identified from the data in **a** is rendered semi-transparent in three different orientations together with examples of five T-cell tracks differentially interacting with this surface. Tracks are labelled at their temporal beginnings. Arrowheads highlight positions where tracks cross the GC surface. ko, knockout; wt, wild type. **c**, Migration patterns of *Sap*$^{+/+}$ and *Sap*$^{-/-}$ T cells that arrived at a 10-μm-wide virtual mantle–GC interface zone. Area between the two dotted circles represents the 10-μm-wide interface zone; inner circle represents the GC surface, whereas the area outside of the outer circle is the follicular mantle. Blue line segment indicates the region in which a track began (that is, the mantle zone (top) or the GC (bottom)). Numbers in blue are the total number of tracks of the indicated type analysed. Three red arrows denote tracks that subsequently moved into the mantle zone, stayed within the interface zone, or moved into the GC, respectively. Corresponding numbers denote percentages of tracks of each genotype that exhibited the indicated behaviour. Data are pooled from three experiments. **d**–**f**, Migration of *Sap*$^{+/+}$ and *Sap*$^{-/-}$ OT-2 T cells in follicles containing non-cognate GCs. **d**, A schematic showing the protocol used to generate GCs that are non-cognate to the OT-2 cells activated in the same lymph node. i.v., intravenous (see Methods for details). BM, bone marrow. **e**, Typical migration patterns of the two types of T cells in the same configuration as in **a** (see also Supplementary Movie 7). **f**, T-cell tracks that came within 10 μm of non-cognate GCs were analysed for their subsequent migrations using the same method as that used in **c**. Data from two experiments are pooled.

Fig. 6), and a virtual mantle–GC interface zone was then defined as encompassing spatial coordinates within 10 μm of the GC outer surface. T-cell tracks were subsequently classified according to their interactions with this interface zone (Fig. 4b, c). When reaching the interface from the follicular mantle, $Sap^{+/+}$ OT-2 T cells were more likely to continue into the GC than to return to the mantle. $Sap^{-/-}$ T cells exhibited the opposite behaviour, being more likely to turn back than to cross into the GC. Conversely, when reaching the interface zone from within the GC, $Sap^{+/+}$ T cells were more likely to return to the GC than to escape into the mantle, whereas $Sap^{-/-}$ T cells were much more likely to escape than to return. For those tracks that started from the interface zone, $Sap^{-/-}$ T cells exhibited a preference for migrating into the mantle compared to moving into the GC, whereas for $Sap^{+/+}$ T cells the movement in these two directions was comparable. Consistent with these distinct migration patterns, $Sap^{-/-}$ T cells also exhibited significantly shorter GC retention times (Supplementary Fig. 7). Therefore, in the absence of SAP, T cells are not efficiently recruited into or retained within a nascent GC. These data suggest SAP-deficient T cells cannot act as effective GC-associated T_{FH} cells to sustain the GC reaction, a defect that would contribute to the profound impairment of GC responses in SAP-deficient hosts.

To address whether the inefficient GC recruitment and retention of $Sap^{-/-}$ T cells resulted from their reduced antigen-specific interactions with B cells, radiation bone-marrow chimaeras were constructed so that endogenous B cells were deficient in MHC class II expression and thus unable to engage in antigen-specific interactions with T cells, whereas T cells could still interact with and be activated by non-B APCs including DCs (Supplementary Fig. 8; see a methodological diagram in Fig. 4d). After co-transfer of both $Sap^{+/+}$ and $Sap^{-/-}$ OT-2 T cells together with MD4 B cells into these chimaeric animals, they were immunized with a mixture of HEL–bovine serum albumin (BSA) and intact OVA proteins. In this setting, MD4 B cells cannot engage transferred OT-2 T cells as cognate partners but can still form GCs (Supplementary Fig. 9a) by using cognate help from endogenous $CD4^+$ T cells. OT-2 cells in these mice can be normally activated by OVA-presenting DCs, but are deprived of cognate interactions with B cells, which are either transferred MD4 cells that do not present OVA or endogenous B cells that are derived from MHC-class-II-deficient bone marrow progenitors. Whereas both $Sap^{+/+}$ and $Sap^{-/-}$ OT-2 T cells upregulated CXCR5 and ICOS expression in this experimental system (Supplementary Fig. 9b), now they both failed to be efficiently recruited into and retained within GCs (Fig. 4e, f, Supplementary Fig. 7 and Supplementary Movies 7 and 8). When the same chimaeric mice were immunized with HEL–OVA, a condition in which OT-2 T cells could engage MD4 B cells as cognate partners, $Sap^{+/+}$ OT-2 T cells were recruited to the GC, whereas $Sap^{-/-}$ OT-2 T cells were not (data not shown). These findings indicate that T cells require cognate interactions with B cells to be recruited into and retained within GCs and suggest that, by failing to engage productively in such cell–cell interactions, SAP-deficient T cells are unable to physically localize to the GC to effectively sustain the GC reaction.

Conclusions

This study demonstrates that SAP expression in T cells is critical for stable antigen-dependent T–B cell adhesion but dispensable for T–DC interactions, revealing that distinct molecular rules govern the stable interactions of $CD4^+$ T cells with two major APC types *in vivo*. Stabilization of T–B cell interactions may rely on a T-cell-autonomous mechanism orchestrated by SAP and its associated SLAM family molecules at the cell–cell interface, whereas stable T–DC association might be actively promoted by means of DC-mediated mechanisms, such as those involving cytoskeletal and membrane mechanics[38,39]. In accordance with this notion, B cells but not DCs express high levels of SLAM (also known as CD150, SLAMF1), CD84, Ly9 (CD229) and Ly108 (SLAMF6) molecules (Supplementary Fig. 10), which are also highly expressed by T cells activated *in vitro* and by T_{FH} cells *in vivo* (ref. 40 and data not shown). The differential SAP regulation of T–DC and T–B cell interactions correlates with our observations that $CD4^+$ T-cell activation *in vivo* is grossly normal irrespective of SAP expression, whereas otherwise competent effector T cells fail to efficiently deliver contact-dependent help to cognate B cells in the absence of SAP. At the cellular level, these results provide a likely explanation for why SAP deficiency specifically impairs T-dependent humoral immunity but leaves intact or even exaggerates cell-mediated immune responses that also require $CD4^+$ T-cell activity[13–15,41,42]. Although additional factors may also contribute to the overall defects of humoral immunity seen in SAP-deficient hosts[43], our results strongly indicate that the predominant mechanism is the disruption of antigen-specific T–B adhesion. Future studies are necessary to determine the molecular basis for how SAP selectively controls cognate T–B association, to identify SAP-associated SLAM family proteins involved in this process, and to elucidate the cascade of intercellular signal exchange that transpires across a stable T–B synapse.

Our findings offer a compelling explanation for the profound impairment of the GC response in SAP-deficient mice and suggest a mechanism contributing to the B-cell-centric pathologies associated with the X-linked lymphoproliferative syndrome. They provide new insights into the operating principles of intercellular communication between T cells and diverse APCs and serve as a striking example of the importance of a direct visualization approach in understanding immune system function *in vivo*.

METHODS SUMMARY

Cell conjugation assay *in vitro*. OT-2 T cells (5×10^5 per well) were incubated for 30 min at 37 °C in 96-well U-bottom plates with DCs (10^6 per well) or lipopolysaccharide (LPS)-activated B cells (2×10^6 per well) that had been pulsed with antigen. Conjugates were enumerated by flow cytometry after the cell mixture was stained at 4 °C for CD4, CD11c (also known as ITGAX) and CD19 and repeatedly washed.

Adoptive transfer, cell phenotyping and intravital imaging. To visualize T–DC interactions (Fig. 1), 2×10^6 OVA_{323}-pulsed DCs per mouse were injected subcutaneously 24 h before intravenous transfer of $Sap^{+/+}$ and $Sap^{-/-}$ T cells (3×10^6 each). Imaging was conducted 12 to 24 h later. To examine activation phenotypes, 10^6 DCs and 2×10^5 GFP-expressing T cells per mouse were used. To visualize interactions between B cells and $Sap^{+/+}$ and $Sap^{-/-}$ T cells in the same lymph node (Fig. 2), 3×10^6 OT-2 T cells of each genotype were co-transferred into mice together with 5×10^6 wild-type B cells. Immunization was performed 12 h before cell transfer, and imaging was conducted 24 to 36 h thereafter. To visualize T–B interactions under non-competitive conditions and to assay T and B cell expansion (Fig. 3), 6×10^4 GFP-expressing OT-2 T cells were co-transferred together with 3×10^5 CFP-expressing B cells 24 h before immunization. Imaging and cytometric analyses were conducted 60–72 and 96 h later, respectively. To visualize GC recruitment and retention of T cells (Fig. 4), 3×10^4 CFP-expressing $Sap^{+/+}$ and 3×10^4 GFP-expressing $Sap^{-/-}$ OT-2 T cells were co-transferred with 3×10^5 non-fluorescent MD4 B cells. Imaging was conducted 6 to 8 days post immunization. Dye-labelled naive B cells ($2–4 \times 10^7$) were given 1 day before imaging to provide follicle and GC landmarks. The imaging set-up was essentially as described previously[44]. For imaging sessions longer than 2 h, the animal's hydration was maintained by lactated Ringer's solution given by means of a catheter. The typical $x \times y \times z$ dimension was 0.5–1.1 × 0.5–1.1 × 3 μm, and the time resolution was 30–45 s. For experiments involving co-transfer of two types of dye-labelled T cells, the cells were always reciprocally labelled to control for potential dye-induced behavioural differences.

Statistical analysis. The Mann–Whitney rank sum test was used to calculate *P* values for highly skewed distributions. For Gaussian-like distributions, two-tailed *t*-tests were used.

Full Methods and any associated references are available in the online version of the paper at www.nature.com/nature.

Received 8 July; accepted 15 August 2008.

1. Coico, R. F., Bhogal, B. S. & Thorbecke, G. J. Relationship of germinal centers in lymphoid tissue to immunologic memory. VI. Transfer of B cell memory with

lymph node cells fractionated according to their receptors for peanut agglutinin. *J. Immunol.* **131,** 2254–2257 (1983).
2. Berek, C., Berger, A. & Apel, M. Maturation of the immune response in germinal centers. *Cell* **67,** 1121–1129 (1991).
3. Jacob, J., Kelsoe, G., Rajewsky, K. & Weiss, U. Intraclonal generation of antibody mutants in germinal centres. *Nature* **354,** 389–392 (1991).
4. MacLennan, I. C. *et al.* The changing preference of T and B cells for partners as T-dependent antibody responses develop. *Immunol. Rev.* **156,** 53–66 (1997).
5. Raff, M. C. Role of thymus-derived lymphocytes in the secondary humoral immune response in mice. *Nature* **226,** 1257–1258 (1970).
6. Mitchison, N. A. The carrier effect in the secondary response to hapten–protein conjugates. II. Cellular cooperation. *Eur. J. Immunol.* **1,** 18–27 (1971).
7. Lanzavecchia, A. Antigen-specific interaction between T and B cells. *Nature* **314,** 537–539 (1985).
8. Garside, P. *et al.* Visualization of specific B and T lymphocyte interactions in the lymph node. *Science* **281,** 96–99 (1998).
9. Vinuesa, C. G., Tangye, S. G., Moser, B. & Mackay, C. R. Follicular B helper T cells in antibody responses and autoimmunity. *Nature Rev. Immunol.* **5,** 853–865 (2005).
10. Purtilo, D. T., Cassel, C. K., Yang, J. P. & Harper, R. X-linked recessive progressive combined variable immunodeficiency (Duncan's disease). *Lancet* **305,** 935–940 (1975).
11. Grierson, H. L. *et al.* Immunoglobulin class and subclass deficiencies prior to Epstein–Barr virus infection in males with X-linked lymphoproliferative disease. *Am. J. Med. Genet.* **40,** 294–297 (1991).
12. Ma, C. S., Nichols, K. E. & Tangye, S. G. Regulation of cellular and humoral immune responses by the SLAM and SAP families of molecules. *Annu. Rev. Immunol.* **25,** 337–379 (2007).
13. Wu, C. *et al.* SAP controls T cell responses to virus and terminal differentiation of TH2 cells. *Nature Immunol.* **2,** 410–414 (2001).
14. Czar, M. J. *et al.* Altered lymphocyte responses and cytokine production in mice deficient in the X-linked lymphoproliferative disease gene *SH2D1A/DSHP/SAP*. *Proc. Natl Acad. Sci. USA* **98,** 7449–7454 (2001).
15. Crotty, S. *et al.* SAP is required for generating long-term humoral immunity. *Nature* **421,** 282–287 (2003).
16. Morra, M. *et al.* Defective B cell responses in the absence of *SH2D1A*. *Proc. Natl Acad. Sci. USA* **102,** 4819–4823 (2005).
17. Cannons, J. L. *et al.* SAP regulates T cell-mediated help for humoral immunity by a mechanism distinct from cytokine regulation. *J. Exp. Med.* **203,** 1551–1565 (2006).
18. Coffey, A. J. *et al.* Host response to EBV infection in X-linked lymphoproliferative disease results from mutations in an SH2-domain encoding gene. *Nature Genet.* **20,** 129–135 (1998).
19. Sayos, J. *et al.* The X-linked lymphoproliferative-disease gene product SAP regulates signals induced through the co-receptor SLAM. *Nature* **395,** 462–469 (1998).
20. Cannons, J. L. *et al.* SAP regulates T_H2 differentiation and PKC-θ-mediated activation of NF-κB1. *Immunity* **21,** 693–706 (2004).
21. Dent, A. L., Hu-Li, J., Paul, W. E. & Staudt, L. M. T helper type 2 inflammatory disease in the absence of interleukin 4 and transcription factor STAT6. *Proc. Natl Acad. Sci. USA* **95,** 13823–13828 (1998).
22. Andoh, A. *et al.* Absence of interleukin-4 enhances germinal center reaction in secondary immune response. *Immunol. Lett.* **73,** 35–41 (2000).
23. Huang, A. Y., Qi, H. & Germain, R. N. Illuminating the landscape of *in vivo* immunity: insights from dynamic *in situ* imaging of secondary lymphoid tissues. *Immunity* **21,** 331–339 (2004).
24. Stoll, S., Delon, J., Brotz, T. M. & Germain, R. N. Dynamic imaging of T cell–dendritic cell interactions in lymph nodes. *Science* **296,** 1873–1876 (2002).
25. Mempel, T. R., Henrickson, S. E. & Von Andrian, U. H. T-cell priming by dendritic cells in lymph nodes occurs in three distinct phases. *Nature* **427,** 154–159 (2004).
26. Miller, M. J., Safrina, O., Parker, I. & Cahalan, M. D. Imaging the single cell dynamics of $CD4^+$ T cell activation by dendritic cells in lymph nodes. *J. Exp. Med.* **200,** 847–856 (2004).
27. Celli, S., Lemaitre, F. & Bousso, P. Real-time manipulation of T cell–dendritic cell interactions *in vivo* reveals the importance of prolonged contacts for $CD4^+$ T cell activation. *Immunity* **27,** 625–634 (2007).
28. Abbas, A. K., Haber, S. & Rock, K. L. Antigen presentation by hapten-specific B lymphocytes. II. Specificity and properties of antigen-presenting B lymphocytes, and function of immunoglobulin receptors. *J. Immunol.* **135,** 1661–1667 (1985).
29. Okada, T. *et al.* Antigen-engaged B cells undergo chemotaxis toward the T zone and form motile conjugates with helper T cells. *PLoS Biol.* **3,** e150 (2005).
30. Davidson, D. *et al.* Genetic evidence linking SAP, the X-linked lymphoproliferative gene product, to Src-related kinase FynT in T_H2 cytokine regulation. *Immunity* **21,** 707–717 (2004).
31. McCausland, M. M. *et al.* SAP regulation of follicular helper CD4 T cell development and humoral immunity is independent of SLAM and Fyn kinase. *J. Immunol.* **178,** 817–828 (2007).
32. Garcia, Z. *et al.* Competition for antigen determines the stability of T cell–dendritic cell interactions during clonal expansion. *Proc. Natl Acad. Sci. USA* **104,** 4553–4558 (2007).
33. Kelsoe, G. & Zheng, B. Sites of B-cell activation *in vivo*. *Curr. Opin. Immunol.* **5,** 418–422 (1993).
34. Liu, Y. J. *et al.* Sites of specific B cell activation in primary and secondary responses to T cell-dependent and T cell-independent antigens. *Eur. J. Immunol.* **21,** 2951–2962 (1991).
35. Moser, B., Schaerli, P. & Loetscher, P. $CXCR5^+$ T cells: follicular homing takes center stage in T-helper-cell responses. *Trends Immunol.* **23,** 250–254 (2002).
36. de Vinuesa, C. G. *et al.* Germinal centers without T cells. *J. Exp. Med.* **191,** 485–494 (2000).
37. Schwickert, T. A. *et al. In vivo* imaging of germinal centres reveals a dynamic open structure. *Nature* **446,** 83–87 (2007).
38. Al-Alwan, M. M., Rowden, G., Lee, T. D. & West, K. A. The dendritic cell cytoskeleton is critical for the formation of the immunological synapse. *J. Immunol.* **166,** 1452–1456 (2001).
39. Benvenuti, F. *et al.* Requirement of Rac1 and Rac2 expression by mature dendritic cells for T cell priming. *Science* **305,** 1150–1153 (2004).
40. Chtanova, T. *et al.* T follicular helper cells express a distinctive transcriptional profile, reflecting their role as non-Th1/Th2 effector cells that provide help for B cells. *J. Immunol.* **173,** 68–78 (2004).
41. Hron, J. D. *et al. SH2D1A* regulates T-dependent humoral autoimmunity. *J. Exp. Med.* **200,** 261–266 (2004).
42. Crotty, S. *et al.* Hypogammaglobulinemia and exacerbated CD8 T-cell-mediated immunopathology in SAP-deficient mice with chronic LCMV infection mimics human XLP disease. *Blood* **108,** 3085–3093 (2006).
43. Ma, C. S. *et al.* Impaired humoral immunity in X-linked lymphoproliferative disease is associated with defective IL-10 production by $CD4^+$ T cells. *J. Clin. Invest.* **115,** 1049–1059 (2005).
44. Qi, H., Egen, J. G., Huang, A. Y. & Germain, R. N. Extrafollicular activation of lymph node B cells by antigen-bearing dendritic cells. *Science* **312,** 1672–1676 (2006).

Supplementary Information is linked to the online version of the paper at www.nature.com/nature.

Acknowledgements H.Q. is in debt to Y. Hong for support, encouragement and inspiration. This work was funded by the intramural research programs of the National Institute of Allergy and Infectious Disease and National Human Genome Research Institute, National Institutes of Health, USA.

Author Contributions H.Q. and J.C. conducted the experiments. R.N.G. and P.L.S. contributed equally to this study. All authors contributed collectively to designing the experiments, interpreting the data and writing the paper.

Author Information Reprints and permissions information is available at www.nature.com/reprints. Correspondence and requests for materials should be addressed to R.N.G. (rgermain@niaid.nih.gov) or P.L.S. (pams@nhgri.nih.gov).

METHODS

Mice. SAP-deficient mice were described previously[14] and backcrossed to B6 for at least ten generations. B6 (Jax 664), CD45.1 congenic (Jax 2014), HEL-specific Ig-transgenic MD4 (Jax 2595), μMT (Jax 2288), GFP-expressing (Jax 4353), CFP-expressing (Jax 4218) and $OVA_{323–339}$-specific TCR-transgenic OT-2 (Jax 4194) mice were purchased from the Jackson Laboratory. I–$A\beta^{-/-}$ mice were purchased from Taconic Farms. Relevant mice were interbred to obtain CFP–MD4, $Sap^{+/+}$ CFP–OT-2, and $Sap^{+/+}$ or $Sap^{-/-}$ GF–OT-2 mice. All mice were maintained under specific-pathogen free conditions, and used in accordance of NIH institutional guidelines for animal welfare.

Cell preparation, antigen generation and immunization. To isolate DCs, mouse spleens were digested with 400 μg ml^{-1} Liberase CI and 20 μg ml^{-1} DNase I for 30 min (Roche) before subjected to CD11c microbeads-based isolation protocol (Miltenyi Biotec). DCs were pulsed with indicated doses of OVA_{323} peptide antigen in the presence of LPS for 2 h, washed, and used for the *in vitro* cell conjugation assay or for subcutaneous injection into mice after being labelled with 75 μM Cell Tracker Blue (CMF_2HC). OT-2 T cells and B cells of either a MD4 or a polyclonal repertoire were isolated by CD4 T-cell isolation kit and naive B-cell isolation kit (Miltenyi Biotec), respectively. For intravital imaging experiments involving dye-labelled cells, the MD4 B cells were always labelled with 75 μM CMF_2HC, whereas $Sap^{+/+}$ and $Sap^{-/-}$ OT-2 T cells were interchangeably labelled with either 2 μM carboxyfluorescein diacetate succinimidyl ester (CFSE) or 4 μM Cell Tracker Red (CMTPX). All dyes were purchased from Invitrogen. Model antigens used for subcutaneous immunization included OVA protein and chemical conjugates of OVA and HEL or BSA and HEL. The purified proteins were purchased form Sigma-Aldrich, and conjugates were made with the HydraLink heterobifunctional conjugation kit (SoluLink) according to manufacturer's instructions. In brief, HEL was modified by 6-hydrazinonicotinamide and then allowed to react at a molar ratio of 5:1 with OVA or BSA that was modified by 4-formylbenzoate. Excessive unconjugated HEL was then removed by size-exclusion chromatography. Mice were immunized with the indicated antigen mixed with alum and 0.2 μg LPS.

Transient transfection of T cells. For certain experiments, blasting OT-2 T cells were transfected with 4 μg DNA constructs expressing GFP-tagged SAP or GFP alone by an Amaxa nucleofector (program X-001) before being analysed for conjugation formation with B cells. Reconstituted expression of SAP proteins in $Sap^{-/-}$ T cells was verified by western blotting.

Construction of mixed bone marrow chimaeras. B6 or CD45.1 congenic mice were lethally irradiated by γ-ray from a cesium source (900 rad) and then received intravenous transfer of a total of 1.25×10^5 bone-marrow-lineage-negative cells, which were isolated using the mouse lineage depletion kit (Miltenyi Biotec). To make chimaeric mice that lacked MHC class II, a mixture of 80% μMT and 20% I–$A\beta^{-/-}$ donor bone marrow cells were used. For certain control experiments, I–$A\beta^{-/-}$ donor cells were replaced with regular B6 cells.

Flow cytometry and immunohistochemistry. All reagents were purchased from BD Pharmingen unless indicated otherwise. To examine surface phenotypes of OT-2 T cells or MD4 B cells, draining lymph node cells were washed, incubated with 50 μg ml^{-1} rat and hamster IgG whole molecules (Pierce) and 10% 2.4G2 hybridoma supernatants, and then stained with indicated antibodies in PBS supplemented with 2 mM EDTA and 0.5% fetal calf serum. Staining reagents included AlexaFluor 700 anti-CD4 (eBioscience), AlexaFluor 700 CD38 (eBioscience), APC-Cy7 anti-CD19, phycoerythrin (PE) anti-Fas, PE anti-ICOS, PE anti-OX40, PE anti-I–Aβ, APC anti-CD11c, biotinylated anti-CD40L, biotinylated anti-CXCR5, biotinylated anti-IgM^a, 7-AAD, streptavidin APC, and isotype-matched non-specific antibodies. Cells were stained on ice with primary reagents for 1 h and with the secondary reagent for 20 min. Cytometric data were collected on an LSR II cytometer (BD) and analysed with FlowJo software (TreeStar). Dying cells and cell multiplets were excluded from analysis based on 7-AAD fluorescence and forward-scattering intensity (FSC)-height/FSC-area. Quantitative analysis of cell surface phenotypes involved determining percentages of positive cells based on a cutoff established by the isotype control (for CXCR5 and CD40L) or by calculating the normalized expression level based on geometric mean fluorescence intensities ($\log_{10}(MFI^{sample})/\log_{10}(MFI^{isotype})$ for ICOS and OX40). For immunohistochemical staining of lymph node sections, the protocol was as described previously[44]. Staining reagents included AlexaFluor 647 anti-B220, biotinylated anti-IgD, purified GL7 (eBioscience), AlexaFluor 647 anti-rat IgM (Invitrogen) and streptavidin AlexaFluor 568 (Invitrogen). All stained slides were mounted with ProlongGold antifade reagents (Invitrogen) and examined with a Leica TCS SP5 confocal system.

Intravital imaging and quantitative data analysis. To maintain consistency of visual presentation in all figures and movies, the $Sap^{+/+}$ and $Sap^{-/-}$ T cells were pseudo-coloured in red and green, respectively. An excitation wavelength between 783 and 800 nm was used for dye-labelled cells. For imaging experiments involving GFP- or CFP-expressing transgenic T or B cells, with or without additional CMTPX-labelled naive B cells, an excitation wavelength between 840 and 850 nm was used, a compromise wavelength for simultaneous visualization of CFP and GFP or all of the three fluorochromes. Whereas the overlap between normalized emission curves of CFP and GFP is substantial, the GFP transgenic line used here (Jax 4353, Jackson Laboratory) is ~100 times 'brighter' than the CFP transgenic line (Jax 4218, Jackson Laboratory), allowing real GFP signals to be readily distinguished from bleed-through signals from CFP. Post data acquisition, four-dimensional image data sets were analysed using Bitplane Imaris software package. Cell–cell contacts were scored manually in blind analyses. Cell migration was analysed through automatic cell tracking aided by manual supervision. Only cell tracks that lasted longer than 5 min were included in quantitative analysis. For certain experiments, it was necessary to quantitatively analyse cell positioning over time in relationship to the GC in space. To achieve this, the boundary of GC was manually traced for each optical slice in a time-averaged series and then mathematically defined as a triangulated surface in three-dimensional space by an optimized Dirichlet tessellation algorithm implemented in C++ (F.K. *et al.*, manuscript in preparation). The distance from a cell at any give time to the GC surface can then be calculated (see Supplementary Fig. 6 for a flow chart of the relevant data processing). For all imaging experiments, final presentations of time-lapse image sequences as stills or movies were created using Photoshop, AfterEffect and Illustrator (Adobe).